New Indices for Detection of Turbine blade Tip Deformation and Estimation of Clearance Extent Using Scattering Parameter

Mehdi Aslinezhad[1] **Maryam A. Hejazi** [2]
[1] Ph.D. Student, Electrical and Computer Engineering Department University of Kashan, Kashan, Iran
maslinejad@yahoo.com
[2] Assistant Professor, Electrical and Computer Engineering Department University of Kashan, Kashan, Iran
mhejazi@ kashanu.ac.ir

Abstract :

Reliability of gas turbine power plant is related to the blade normal operation. In this paper, a new on-line condition monitoring method has been presented to evaluate two important factors affecting the turbine blades that are the tip clearance and tip deformation.
A K band's microwave sensor has been simulated and optimized in CST Microwave Studio software. Scattering parameters of the near field sensor has been used as a finger print for the turbine blade. A set of measuring indices has been introduced to compare the amplitude and phase of the scattering parameters and received power. The simulation results show that the proposed indices can effectively detect deformation of the blade tip and tip clearance extent can also be estimated.

Keywords: Tip clearance, Measuring indices, K band's microwave sensor, Scattering parameters

Submission date:04, 12, 2018

Acceptance date:20, 08, 2018

Corresponding author: Maryam A. Hejazi

Corresponding author's address:6 Km Ravandi Blvd.Elec. Eng. Dep., University of Kashan, Kashan, Iran

1. Introduction

Reliability enhancement of gas turbine power plant is a key factor in the resiliency of power network. On-line condition monitoring of its important elements like turbine is a known method for reliability improvement. The availability of gas turbine is strongly associated with its parts reliability and maintenance policy [1].

A number of studies have reported that 42% of gas turbine failures are due to the defection of the turbine blade. Therefore, the blade is a limiting element for gas turbines [2]. Gas turbine blades are critical components in power plants which in the event of their failure the power plant will shut down. This case can cause long time power failure and economic loss. Therefore, it is necessary to study the failure analysis of turbine blades in order to increase the reliability of power systems [3]. Increase in pressure and centrifugal force, high vibrations caused by pressure in the inlet, collision of external objects with turbine blades, non-synchronization of vibrations due to defection in fuel system, sedimentation and corrosion due to high-pressure and high temperatures gases which can reach to 800 to 1200 ^{o}C, and chipping and fracture of turbine blade due to exhaustion and over temperature are the factors causing defect in turbine blades and rendering gas turbines out of order. Any of these events can decrease stability of the turbine blades and alter tip clearance and blade shape which has been shown in Fig .1[4,5].

(a) (b)

Fig.1. Types of failures in the turbine blade (a) Tip clearance decrease (b) Blade deformation

There is always an inverse relationship between the turbine engine efficiency and the tip clearance and it has been repeatedly reported that the 0.0254mm reduction in this distance could increase the engine efficiency by 0.1% [6].

Because a wide tip clearance will allow high-pressure and hot gases to escape from the main path and eventually reduces engine efficiency. On the other hand, a great reduction of this distance will increase the risk of rubbing the tip of the blade to the shell and, finally, the engine will collapse [7]. In order to maintain a balance in the amount of distance between the blade tip and the shell, this distance should be continuously monitored and controlled. When the tip clearance of the blade reaches the warning stage, the turbine speed should decrease by limiting the amount of fuel fed to the turbine [8].

Gas turbine monitoring means to monitor the performance of its various parts in order to prevent defect or timely detection of the defect. Many operators are keen to know the state of the inside of the turbine, because the turbine blades health monitoring in operation mode prevents excessive costs for over haul and reduces maintenance costs, increases the life span of the turbine, prompts quick and timely action to correct small defects and prevent it from spreading to other parts of the gas turbine. In this way, by preventing serious damage to turbine blades, timely information can be used to increase its reliability.

Gas turbine monitoring means to monitor the performance of its various parts in order to prevent defect or timely detection of the defect. Many operators are keen to know the state of the inside of the turbine, because the turbine blades health monitoring in operation mode prevents excessive costs for over haul and reduces maintenance costs, increases the life span of the turbine, prompts quick and timely action to correct small defects and prevent it from spreading to other parts of the gas turbine. In this way, by preventing serious damage to turbine blades, timely information can be used to increase its reliability.

The advanced gas turbine health monitoring methods are classified into model based diagnosis, such as observers, parity equations, parameter estimation and Gas Path Analysis (GPA)) and also software computing diagnosis such as expert system, fuzzy logic, Neural Networks (NNs) and Genetic Algorithm (GA) [9]. An introduction, advantages, and disadvantages of each advanced engine health monitoring methods are presented in [10,11].

There are also many efforts to monitor and evaluate the health of blades by using optical, inductive, capacitive and microwave sensors. Optical sensors have small size, good time accuracy, high resolution and sufficient bandwidth. However, high operating temperature of the turbine, as well as smoke particles and debris in the gas medium make optical sensors unsuitable for many aero engines and gas turbines [12].

Capacitive sensors can withstand high temperatures but they are sensitive to dielectric changes of gas and have a limited bandwidth and inductive sensors are only able to sense ferromagnetic materials that are rarely used in modern gas turbines [12, 13,14].

Recently, several sensors have been used simultaneously to measuring the tip clearance [15].

Microwave sensors are a promising technology to overcome these limitations. Microwave sensors are not sensitive to a polluted medium and have a sufficiently large bandwidth. They are also resistant to high temperatures.

Different types of microwave sensors are designed and developed to measure tip clearance and tip timing of the blades [16-19].

The novelty of this research is in the method proposed for interpreting the signal received by microwave sensor which is proposed measuring indices for

comparison of scattering parameters. This paper will be presented in three sections:
Initially, a microwave antenna sensor for detecting blade faults has been simulated and optimized in the near field by CST Microwave Studio software.
The next section discusses the method of extracting the amplitude and phase of the scattering parameter and the received power from the sensor as indices for detection of the blade defect and its extent due to change in tip clearance and blade deformation which may occur during the operation of the gas turbine.
Finally, a variety of measuring indices have been extracted and evaluated to estimate the defect and its extent. In this method, the measuring indices are like fingerprint of a turbine blade and are compared for defect detection.
In this monitoring method which is based on extracting the defect extent using measuring indices, the type of received characteristic such as amplitude and phase of the scattering parameter, as well as the received power by the sensor, have a significant effect on the form of the measurement index. And the database of these indicators has the simulation information in the healthy and defective state of the turbine blades.

2. Microwave Antenna Sensor Design

The antennas according to their application and environment can be wired, waveguide, aperture, micro strip, dish in single or multiple arrays and in different sizes. One of the basic things about antennas is their center frequency and bandwidth.
Each antenna is designed to propagate in certain frequency band. The region of propagation of electromagnetic waves around an antenna is divided up into three fields that have different characteristics. Far field region, radiating near field region and reactive near field region. The boundary of the reactive near field region (R) can be calculated from (1).

$$0.62\sqrt{\frac{D^3}{\lambda}} > R \qquad (1)$$

Where D is the largest antenna dimension and λ is wavelength. The reactive near field region usually is not considered as an operational area, but its features can be used as a tool for detecting turbine blades that are located very close to the shell.
The antenna structure of this design is a very small open-ended microwave cavity resonator that operate in the reactive near field region as a short range radar system [20,21].
This sensor must be resistant to extreme heat and to prevent to be affected by high pressure and high temperature gases inside the turbine space and to prevent entering contaminants, the aperture is covered by a protective ceramic cap with a relatively high dielectric coefficient to adapt microwave circuit to propagation environment along with antenna protection from entering hot gases.
Resonance frequency of the cavity is related to temperature because the dielectric constant of the ceramic hood changes by temperature. The relationship between the dielectric coefficient and temperature should be known to consider the change in the scattering parameters and resonance frequency only due to dynamic variation of turbine blades, otherwise temperature should be constant.
The resonator diameter should be smaller than the distance between two neighboring blades and comparable with the thickness of the blade leaf [22].
The circular antenna has been designed and simulated in CST Microwave Studio software in the range of 22 to 27 GHz. First, numerical analysis of the circular cavity resonator in the dominant mode, resonance frequency (f_r) and its cutoff frequency (f_c) are performed by solving the Maxwell equations, after that, with respect to the feeding of resonator by coaxial cable from the lateral side of cavity for excitation of TE_{11} mode, location of the cable and optimal antenna length (L) has been determined [23].
The transverse field components of the TE_{nm} modes for plus z-directed waves in the circular waveguide is as follows

$$E_r = jH0\frac{nw\mu}{Kc^2 r}e^{-j\beta z}\, j_n(Kc\,r)\sin n\phi$$
$$E_\phi = jH0\frac{w\mu}{Kc}e^{-j\beta z}\, j'_n(Kc\,r)\cos n\phi \qquad (1)$$

Where $K_c = {q'_{nm}}/{a}$ and q'_{nm} represent the m[th] root of the Bessel function ($j_n'(n) = 0$), by choosing the dominant mode for the circular waveguide resonator the cutoff frequency of the waveguide is equal to

$$f_c = \frac{q'_{nm}\times c}{2\times\pi\times a} \qquad (3)$$

Which in the TE_{11}mode, q'_{nm}=1.8412, a is the radius of the cavity and c is the wave velocity [24]. Also, the wavelength of the waveguide (λ_c) is proportional to its diameter (D).

$$\lambda_c = K_{nm}\times D \qquad (4)$$

The value of K_{nm} and the resonance wavelength λ_r are calculated by the following equation:

$$K_{nm} = \frac{\pi}{q'_{nm}} \qquad (5)$$

$$\lambda_r = 1/\sqrt{(1/K_{nm}.D)^2 + (p/2.l)^2} \qquad (6)$$

Where p is the number of half-wave field variations in the z direction, K_{mn} in TE_{11} mode is equal to 1.706 [24], D is diameter of the cavity and l is the cavity resonator length. Therefore, by numerical analysis of the microwave circular waveguide in the K band and the software optimization for the resonance frequency 24 GHZ and taking into account the relatively high dielectric constant of the resonator cap at its open end,

the diameter of the cavity resonator is D = 8.5mm and its length is l=12mm (Fig. 3).

The sensor is powered by a coaxial cable from the back of the cavity, which, using its internal conductor, can transfer the waves in the cavity resonator.

In this research, monitoring is based on the analysis of the scattering parameters and resonance frequency variation in the reactive near field of the antenna, so the tip of the blade is placed at a distance of less than λ/2 from the antenna and the blade is part of the antenna's resonance circuit and the crossing of the blade in front of the antenna field causes this circuit to reset.

The sensor designed in this project has a reactive near field boundary of 4mm and the tip of the blade in the standard state is located at 2mm from the sensor.

The transmitted wave which is the reference wave has a phase of θ_0 and the reflected wave from the blade weakened and has a phase shift compared to the reference wave which shown in Fig .2 andcan be obtained as follows:

$$\theta_{relative} = \theta_0 + (\frac{2d}{\lambda}).2\pi \qquad (7)$$

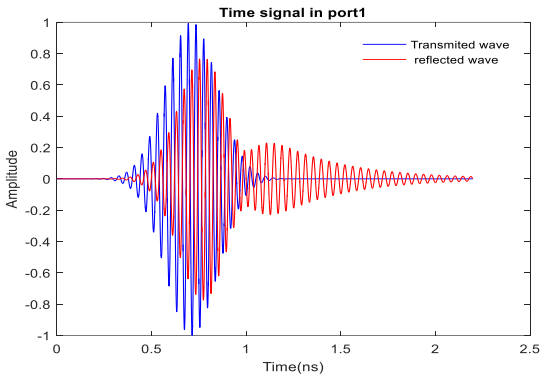

Fig. 2. Voltage drop and phase shifts of the reflected wave from the blade relative to the reference wavelength

In later sections, using the theory of small perturbations and simulation, the effects of blade displacement and deformation on the scattering parameter and resonance frequency are shown.

3. Blade Monitoring Using Scattering Parameters

The matrix that describes the flow of energy between different points of a microwave network is called scattering parameter S.

$$[V^-]=[S]\times[V^+] \qquad (8)$$

Fig. 3 shows the sensor which is an antenna designed and optimized in the K band frequency with coaxial feed and is located in the proximity of the turbine blades as an n port network.

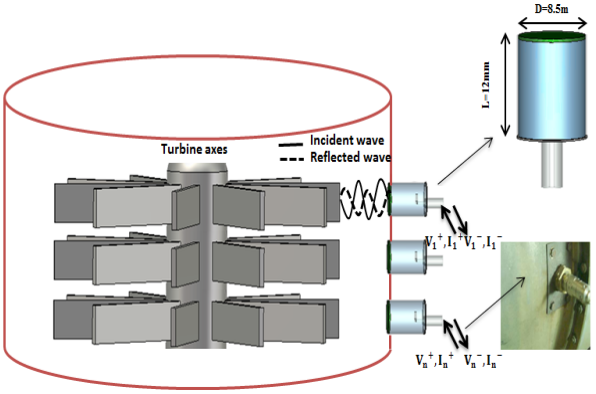

Fig. 3.Turbine model as an n port network

If a wave with the amplitude V_1^+enters this sphere, a reflection wave with $V_1^- = S_{11}V_1^+$ amplitude in line (1) is created that S_{11} is ,in fact, the reflection coefficient and some waves are dispersed and appeared in other ports which their amplitude are proportional to the amplitude$V_1^+.V_n^- = S_{n1}V_1^+$which $S_{n1}$is,in fact, the transfer coefficient from port 1 to port n.

If the incident waves radiate to all ports, then:

$$\begin{bmatrix} V^-_1 \\ V^-_2 \\ . \\ . \\ . \\ V^-_n \end{bmatrix} = \begin{bmatrix} S_{11} & S_{12} & . & . & . & S_{1N} \\ S_{21} & S_{22} & . & . & . & S_{2N} \\ . & . & . & . & . & . \\ . & . & & . & . & . \\ . & . & . & . & . & . \\ S_{N1} & S_{N2} & . & . & . & S_{NN} \end{bmatrix} \begin{bmatrix} V^+_1 \\ V^+_2 \\ . \\ . \\ . \\ V^+_n \end{bmatrix} \qquad (9)$$

The system designed in this paper has one antenna which is both input and output, so the scattering matrix consists of only one element, in which case:

$$S11 = \frac{V_1^-}{V_1^+} \qquad (10)$$

Considering the turbine chamber as a cavity resonator, the sensitivity of the scattering parameter to displacement and deformation of the tip of the turbine blades is justifiable by the theory of small perturbation in a cavity resonator. A cavity resonator is made of any enclosed space that is surrounded by a metal surface with a high conductivity. Maxwell's equations must be solved considering the boundary conditions of the cavity in order to analyze the electromagnetic fields of the cavity and the resonance frequency.

Fig. 4(a) represents a cavity resonator formed by a conductor covering S and enclosing the loss-free region τ. Fig. 4(b) represents a deformation of original cavity such that the conductor covers $S' = S - \Delta S$ andencloses $\tau' = \tau - \Delta\tau$.

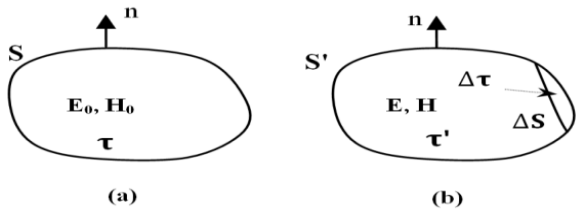

Fig. 4. Perturbation of cavity walls (a) original (b) perturbed cavity

In this paper, the change in the resonance frequency due to the change in the cavity wall is determined. If E_0, H_0 and w_0 represent the field and the resonance frequency of the original cavity, and that E, H and w represent the corresponding quantities of the perturbed cavity, in both cases the field equations must be satisfied, that is,

$$\frac{w-w_0}{w_0} \approx \frac{\iiint_{\Delta\tau}(\mu|H_0^2| - \varepsilon|E_0^2|)\,d\tau}{\iiint_{\Delta\tau}(\mu|H_0^2| + \varepsilon|E_0^2|)\,d\tau} \quad (11)$$

$$\frac{w-w_0}{w_0} \approx \frac{\Delta\overline{w}_m - \Delta\overline{w}_e}{w} \quad (12)$$

Where $\Delta\overline{w}_m$ and $\Delta\overline{w}_e$ are time-average electric and magnetic energies originally contained in $\Delta\tau$ and w is the total energy stored in the cavity. If $\Delta\tau$ is of small extent, then the relation can be approximated as follows:

$$\frac{w-w_0}{w_0} \approx \frac{(\overline{w}_m - \overline{w}_e)\Delta\tau}{\hat{w}\tau} = C\frac{\Delta\tau}{\tau} \quad (13)$$

Where $\overline{w}_m$ and $\overline{w}_e$ are respectively the magnetic and electrical energy densities, and $\hat{w}$ is the space-average energy density. Cdepends only on the cavity geometry and the position of the perturbation [25].

Equation (14) shows that the shift of resonance frequency is a function of $\Delta\tau/\tau$. This shows that further changes on the blade have a greater effect on the resonance frequency. Generally, the frequency shift depends on the type of deformation and the shape of the cavity, and the amount of the frequency shift depends on the field in disturbance point. Therefore, the blade's relative position to the sensor, so the blade's tip deformation, can affect the resonance frequency and scattering parameters.

In this paper, two types of faults, namely, the change in the tip clearance, as well as the fracture and deformation of the blade has been simulated, that these defects are different in size. Therefore, with change the amount of $\Delta\tau/\tau$, the scattering parameters and resonance frequency will change in the near field of sensor and will stored in a database for healthy and defective states of blade.

These deformations are simulated in CST Microwave Studio software. The hardware used to simulate the blade and sensor is a computer system with 256 gigabytes of RAM, 18-core processor and processing frequency of 3.6 GHZ. Each simulation has taken 5 hours to complete.

3.1. Change in Tip Clearance

In this research, the standard tip clearance value is considered to be 2mm, and changes from 0.2 to 5mm with a displacement of 0.1mm, in 49 different modes are simulated, and the amplitudes and phases of the scattering parameters are extracted.

In Fig. 5 (a) and (b) for simplicity only 5 of 49 modes (standard modes (2mm), and four values of 1mm, 3mm, 4mm and 5mm) of amplitude and phase of scattering parameter in the desired frequency range are shown.

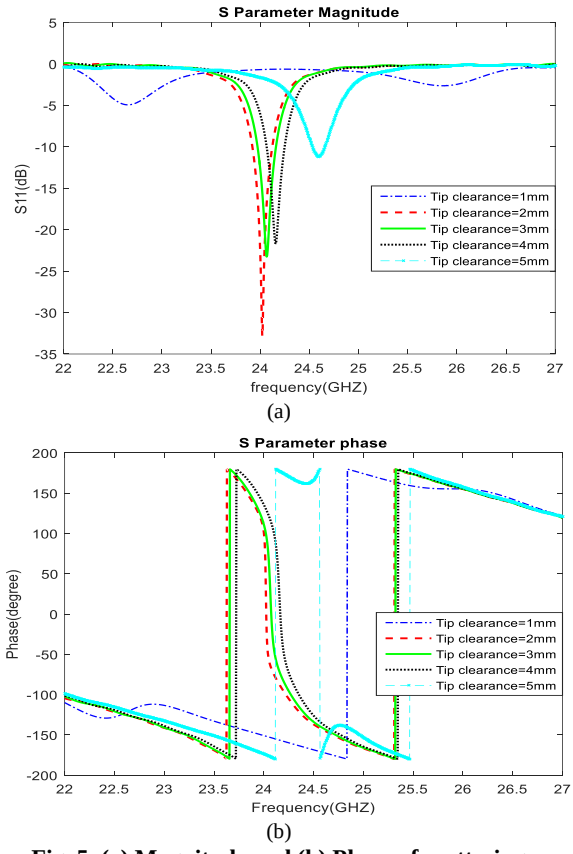

Fig. 5. (a) Magnitude and (b) Phase of scattering parameters due to change in clearance

When the distance of blade tip is 2 mm from the antenna at frequency of 24 GHZ a good adaptation between the sensor and the blade tip exists and the amount of the return signal reaches its minimum. In the above figures it can be seen that by removing the blade from the microwave sensor, the resonance frequency changes and the amount of received power by the sensor decreases and the amplitude of the scattering parameter at the same frequency increases. But considering that the blade is positioned inside the boundary of the near field region (4 mm), the phase

change rate is not symmetric in the different modes of tip clearance decrease and increase.

3.2. Deformation and Fracture of the Turbine Blade Tip

Fig. 6 shows a simulated chipping of the turbine blade tip that may be caused by various factors.

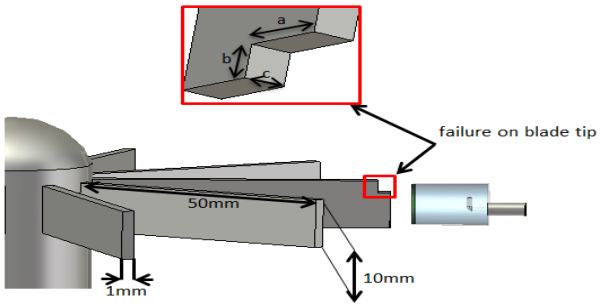

Fig. 6. Simulated turbine blade tip deformation

In Table I, likewise, only 5 types of fracture formed at the tip of the blade are listed.

Table. I. Fractures

Deformation type	NO.1	NO.2	NO.3	NO.4	NO.5
a(mm)	1	2	4	6	8
b(mm)	2	2	2	2	2
C(mm)	2	2	2	2	2
Deformation volume(mm^3)	4	8	16	24	32

Fig. 7(a) to (c) shows the amplitude and phase of the scattering parameter as well as the received power in these 5 deformation types. In these simulations the tip clearance is not changed and is equal to 2mm.

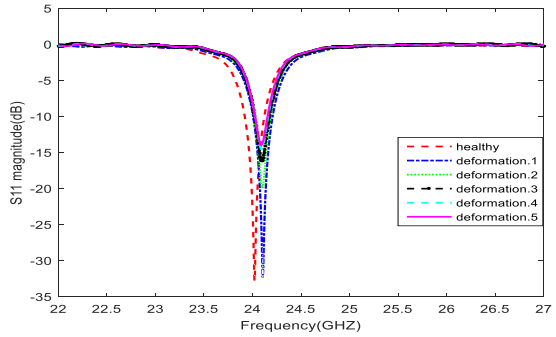

(a)

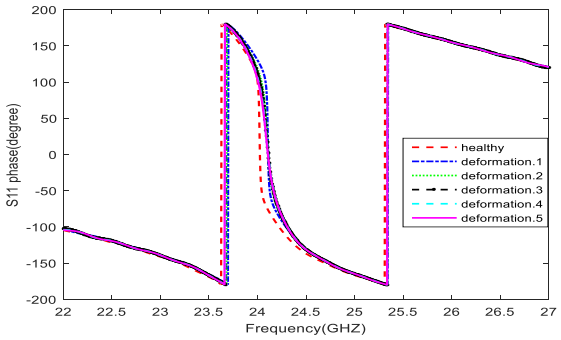

(b)

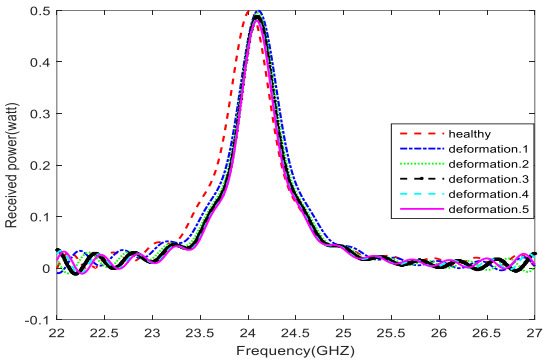

(c)

Fig. 7. (a) S parameter magnitude (b) S parameter phase (c) Received power caused by blade tip deformation and fracture

It should be noted that the number of deformation modes at the tip of the turbine blade is 92, but for simplicity only 5 modes are shown. Here, like in previous modes, the ideal mode is when no deformation occurs in the blade and its distance from the sensor is 2 mm. blade fracture can change resonance frequency and, as the fracture amount increases, S_{11} increases.

4. Failure Detection Using Measuring Indices

The basis of the proposed indices for the detection of gas turbine defects is comparison of the amplitude and phase of the scattering parameter and received power in the unknown and healthy states. These indices are the fingerprint of the turbine blades, and while comparing the amplitude and phase of the scattering parameter and received power of the signal in the healthy state (a blade without deformation and at a distance of 2 mm from the sensor) and the defective state, the defect detect and its value is estimated. It should be noted that the number of samples of the scattering parameters have a significant effect on the accuracy of the indices.

In this research, comparison approach using the measuring indices is based on simulated electromagnetic model of turbine blades and microwave sensor in resonance mode and can estimate the shape and mode of blade defect from the healthy state. Continuous monitoring of the turbine blade by the received scattering parameter from the microwave sensor provides the necessary data for the comparison. In this paper, the basis of detecting the measuring indices is changing the resonance frequency around the frequency range of 22 to 27 GHZ in the scattering parameters and the received power due to the change of cavity resonator (sensor) length because of change in the shape of the blade and the tip clearance.

4.1. Index of Mean Absolute Amplitude, Phase and Received Power Difference

This index is used to compare the amplitude and phase of the scattering parameter as well as the amplitude of the received power in defective and healthy states at N different frequencies. The index of mean absolute magnitude difference (MAMD), mean absolute phase difference (MAPD)[26] and mean absolute received power difference (MARD) for state x respect to reference state are defined as follows:

$$MAMD(x)=\frac{\sum_{i=1}^{N}\left\|S_i(x)\right|-\left|S_i(0)\right\|}{N} \quad (2)$$

$$MAPD(x)=\frac{\sum_{i=1}^{N}\left|\angle S_i(x)-\angle S_i(0)\right|}{N} \quad (3)$$

$$MARD(x)=\frac{\sum_{i=1}^{N}\left\|P_i(x)\right|-\left|P_i(0)\right\|}{N} \quad (4)$$

In which, $|S_i(x)|$ and $|S_i(0)|$ are accordingly amplitude of the scattering parameter in i[th] frequency, $\angle S_i(x)$ and $\angle S_i(0)$ are phase of scattering parameter in i[th] frequency and $|P_i(x)|$ and $|P_i(0)|$ are amplitude of received power in i[th] frequency in state x and reference state respectively.

4.1.1. Estimation of tip clearance extent

Fig. 8 (a) and (b) show MAMD, MAPD and MARD in terms of simulated tip clearance change from 1 to 5 mm for 1001 frequency points (22 to 27 GHZ).

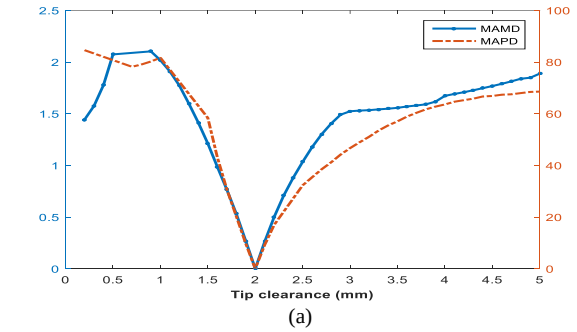

(a)

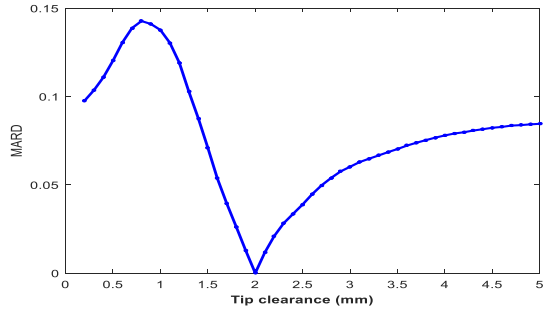

(b)

Fig. 8. (a) MAMD, MAPD and (b) MARD in terms of simulated tip clearance change

The results show that change of tip clearance leads to increase the indices from the reference point (the blade at 2mm distance from the sensor). So they can be used as an indicator for detecting tip clearance and estimating its extent.

4.1.2. Detection of Blade Deformation

The type of deformation in this research is a blade fracture that has been created at the tip of the blade with different volume. Fig. 9 shows the indices MAMD and MAPD for 20 modes of deformation (cavities with different volume in the tip of the blade) for 1001 frequency points from 22 to 27 GHz. The zero point on the horizontal axis is blade healthy point, and since the deformation begins, with increasing deformation the MAPD and MAMD index will increase.

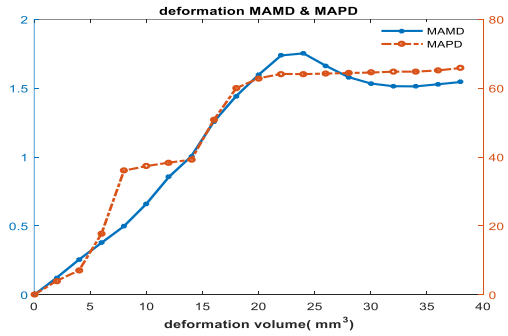

Fig. 9. The values of MAMD & MAPD based on the 20 types of deformation created for the blade

The results show that change of deformation volume leads to increase the indices into the reference point (the blade at 2mm distance from the sensor without deformation). So they can be used as an indicator for detecting deformation.

4.2. Index of Cross-correlation

This index determines the similarity of two wave forms. Similarities in the wave form of amplitude and phase are measured individually. Correlation of the S-parameters Magnitude is defined as follows:

$$CSM(x,0)=corr(\left|S_x\right|,\left|S_0\right|)=\frac{\sum_{i=1}^{N}(\left|S_x(i)\right|-\left|\bar{S}_x\right|)(\left|S_0(i)\right|-\left|\bar{S}_0\right|)}{\sigma_1\sigma_2 N} \quad (5)$$

In the above equation σ_1 and σ_2 are defined as follows:

$$\sigma_1=\left(\frac{\sum_{i=1}^{N}(\left|S_x(i)\right|-\left|\bar{S}_x\right|)^2}{N}\right)^{1/2} \quad (19)$$

$$\sigma_2=\left(\frac{\sum_{i=1}^{N}(\left|S_0(i)\right|-\left|\bar{S}_0\right|)^2}{N}\right)^{1/2} \quad (20)$$

In the above equation CSM(x,0) is the cross-correlation of the amplitude of the scattering parameter for clearance of x mm ($|S_x|$) and reference point ($|S_0|$) and $|S_x(i)|$ is the amplitude of the scattering parameter in ithfrequency, N is the number of points on the frequency axis and $|\bar{S}_x|$ and$|\bar{S}_0|$ are accordingly average scattering parameter in N frequencies in the state x and reference position. In Fig. 10 the value of CSM in term of tip clearance changes is shown.

Correlation of the S-parameters Phase (CSP) is defined as follows:

$$CSP(x,0) = corr(\angle S_x, \angle S_0) = \frac{\sum_{i=1}^{N}(\angle S_x(i) - \angle \bar{S}_x)(\angle S_0(i) - \angle \bar{S}_0)}{\sigma_1 \sigma_2 N} \quad (21)$$

In the above equationσ_1 andσ_2 are defined as follows:

$$\sigma_1 = \left(\frac{\sum_{i=1}^{N}(\angle S_x(i) - \angle \bar{S}_x)^2}{N} \right)^{1/2} \quad (22)$$

$$\sigma_2 = \left(\frac{\sum_{i=1}^{N}(\angle S_0(i) - \angle \bar{S}_0)^2}{N} \right)^{1/2} \quad (23)$$

In the above equation CSP(x,0) is the cross-correlation of the phase of the scattering parameters for moving x mm ($\angle S_x$) and reference point ($\angle S_0$) and$\angle S_x(i)$ is the phase of the scattering parameter in ithfrequency, N is the number of points on the frequency axis and$\angle \bar{S}_x$ and $\angle \bar{S}_0$ are accordingly average scattering parameter in N frequencies in the position x and reference state. In Fig. 10 the value of CSP in term of tip clearance changes is shown.

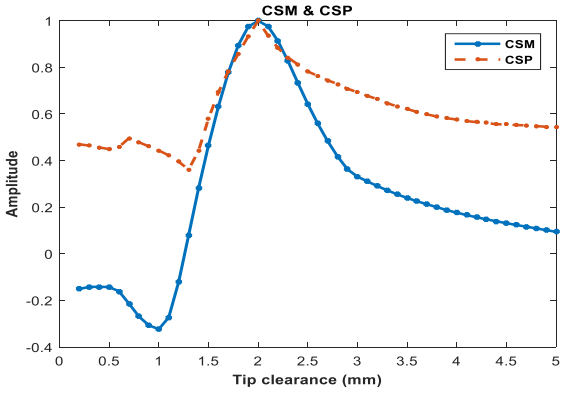

Fig. 10. CSM and CSP based on changes in simulated tip clearance (mm)

The results show that change of tip clearance (increase and decrease) leads to decrease the CSM and CSP indices respect to the reference point (the blade at 2mm distance from the sensor). Therefore, these indices can be used for detecting tip clearance and estimation of its extent. These indexes cannot be used to distinguish the decrease from the increase of tip clearance, because the CSP and CSM are even functions of the displacement. It is clear that at the point of 2 mm the indices have the highest value and the most similarity between the input signals with the reference signal (non-defective state) exists. Fig.11 shows the defect detection algorithm and determines the approximate value of tip clearance by employing indices.

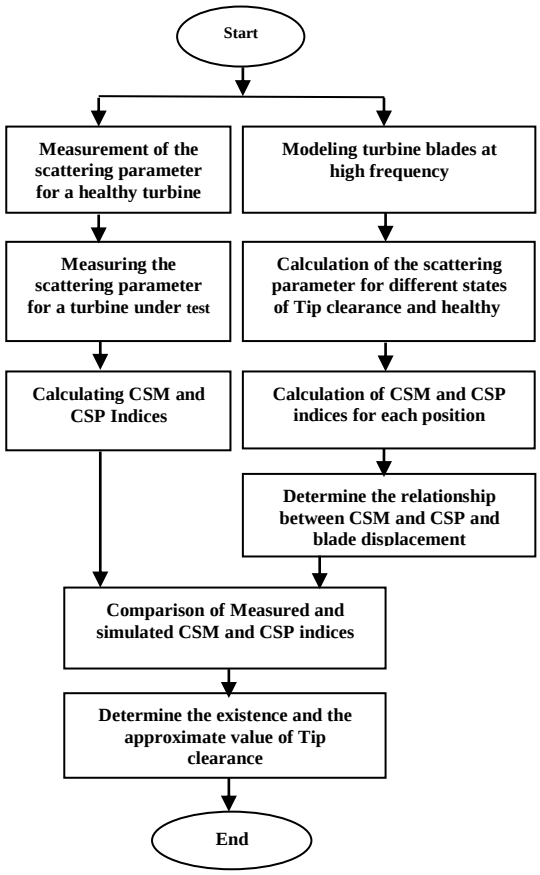

Fig. 11. Detection and determination algorithm of the approximate value of tip clearance using the index

4.3. Euclidean Distance Index

Magnitude Euclidean Distance (MED) and Phase Euclidean Distances (PED) of the scattering parameter, in N different frequencies for the state x to the reference state are respectively defined as follows:

$$MED(x) = \sqrt{\frac{\sum_{i=1}^{N}\left(|S_i(x)| - |S_i(0)|\right)^2}{N}} \quad (24)$$

$$PED(x) = \sqrt{\frac{\sum_{i=1}^{N}\left(\angle S_i(x) - \angle S_i(0)\right)^2}{N}} \quad (25)$$

In which $|S_i(x)|$ and $|S_i(0)|$ are respectively, the amplitude of scattering parameter at the ithfrequency, $\angle S_i(x)$ and $\angle S_i(0)$ are respectively the phase of the scattering parameter at the ith frequency in the state x and reference state.

Fig. 12 shows MED and PED in terms of the simulated tip clearance for 1001 frequency points (22 to 27 GHZ)

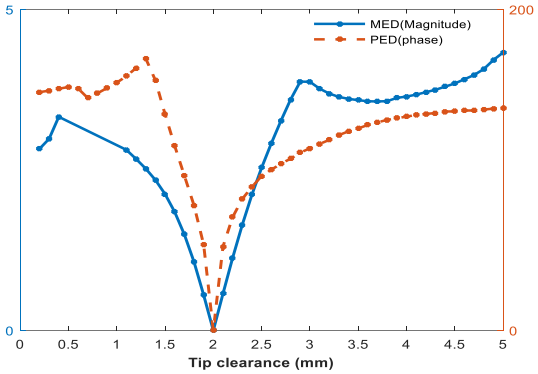

Fig. 12. MED & PED in term of simulated tip clearance change

As shown in Fig.12, MED and PED indices are proportional to the tip clearance change. This means that with decrease and increase of tip clearance the amount of indices will be increased. As a result, they can be used as an index to detect the clearance displacement and estimate its extent, approximately.

5. Conclusion

Due to the particular conditions prevailing in gas turbines, the K-band microwave sensor is proposed to detect mechanical defects in this article. Due to the complex and very large structure of the gas turbine, its electromagnetic modeling will always face very significant problems. Therefore, the proposed method of the use of measuring indices based on the variation of the scattering parameter can be used to extract the faults like the change of tip clearance and deformation of the turbine blades. The important point in this article is the use of scattering parameters in the near field of the sensor and the fact that the tip of the turbine blade is considered a part of the resonance sensor circuit and the smallest changes in the distance of the blade tip to the sensor or shape of the sensor changes the resonance frequency of the sensor, and the methods of extracting these parameters are presented in the body of the present article. Due to the dimensions of the sensor at 24 GHz, the sensor designed in this study has a reactive near field boundary of 4mm and considering that the tip of the blade in the standard state is located at 2mm from the sensor, thus, changes in blade tip and blade defect are also in this distance and using of scattering parameters the defect of blade tip can be detected. Therefore, the method of processing the turbine blade based on electromagnetic waves and measuring indices is a new method in fault finding of gas turbine blades.

References

[1] Fernando Jesus Guevara Carazas, Gilberto Francisco Martha de. Souza," Availability analysis of gas turbines used in power plants, " International Journal of Thermodynamics, Vol. 12 (No. 1), pp. 28-37, March 2009.

[2] V. Naga Bhushana Rao, IN. Niranjan Kumar and K. Bala Prasad, " Failure analysis of gas turbine blades in a gas turbine engine used for marine applications," International Journal of Engineering, Science and Technology, Vol. 6, No. 1 , pp. 43-48, 2014.

[3] RajniDewangan, Jaishri Patel, Jaishri Dubey, Prakash Kumar Sen and Shailendra Kumar Bohidar, "Gas turbines blades a critical review of failure on first and second stages," International Journal of Mechanical Engineering and Robotics Research, Vol. 4, No. 1, January 2015.

[4] N. singh Grewal, "Gas turbine engine performance deterioration modelling and analysis," Ph.D. Thesis, Cranfield Institute of Technology, School of Mechanical Engineering, February 1988.

[5] Hamid Radmanesh, Reza Sharifi, Amin Radmanesh and Seyed Hamid Fathi, "Novel Auxiliary Power Unit Configuration Based On Fuel Cell Technology for Civil Aircraft Application," journal of Iranian Association of Electrical and Electronics Engineers - Vol.14- No.4 Winter 2017.

[6] M. R. Woike, J. W. Roeder, C. E. Hughes, and T. J. Bencic, "Testing of a microwave blade tip clearance sensor at the NASA Glenn research center," in 47th AIAA Aerospace Sciences Meeting, Orlando, Florida 5-8 January, 2009.

[7] N. Goel, A. Kumar, V. Narasimhan, A. Nayak, and A. Srivastava, "Health risk assessment and prognosis of gas turbine blades by simulation and statistical methods," in Proc. Canadian Conference on Electrical and Computer engineering, Niagara Falls on Canada, pp. 1087–1091, May 4-7 2008.

[8] Anwesha Dutta, Shivangi, J. Valarmathi, "Blade tip clearance measurement using microwave sensing system," International Journal of Recent advances in Mechanical Engineering (IJMECH) Vol.4, No.2, May 2015.

[9] M. Aghashabani, J. Milimonfared, A. Kashefi Kaviani and M. Ashabani, "A Neural Network-PSO Based Control for Brushless DC Motors for Minimizing Commutation Torque Ripple,"Journal of Iranian Association of Electrical and Electronics Engineers - Vol.7- No.2- Fall & Winter 2010.

[10] David Kwapisz, MichaëlHafner and Ravi Rajamani," Application of Microwave Sensing to Blade Health Monitoring," infirst European conference of the prognostics and health Management, vol. 3, June 7, 2012.

[11] C Kong and Changduk, " Review on Advanced Health Monitoring Methods for Aero Gas Turbines using Model Based Methods and Artificial Intelligent Methods," International Journal of Aeronautical and Space,vol. 15,pp.123-137,2014.

[12] Jilong Zhang, FajieDuan, GuangyueNiu, Jiajia Jiang and Jie Li, "A blade tip timing method based on a microwave sensor," MDPI Physical Sensors, vol. 17, 11 May 2017.

[13] Thomas Arthur Holst, "Analysis of spatial filtering in phase-based microwave measurements of turbine Blade Tips," A Thesis Presented to The Academic Faculty by Georgia Institute of Technology, August 2005.

[14] Yu Han, Chong Zhong, Xiaoliang Zhu and Jiang Zhe, “Online monitoring of dynamic tip clearance of turbine blades in high temperature environments,” in Measurement Science and Technology, Vol. 29, pp. 1-13, 26 February 2018.

[15] Jose Miguel, Joseba Zubia and Gerardo Aranguren, "Architecture for Measuring Blade Tip Clearance and Time of Arrival with Multiple Sensors in Airplane Engines,” International Journal of Aerospace Engineering, Vol. 2018, 2 May 2018.

[16] J. Geisheimer, S. Billington, T. Holst and D. Burgess, “Performance testing of a microwave tip clearance sensor,” in Proceedings of the AIAA Joint Propulsion Conference, Tucson, AZ, USA, 10–13 July 2005.

[17] Alexander, M. Mikhail and B. Maksim, “Microwave blade tip clearance measurements principles, current practices and future opportunities,” in Proceedings of the ASME Turbo Expo 2012, Copenhagen, Denmark, 11–15 June 2012.

[18] M. Violetti, Q. Xu, O .Hochreutiner and A.K. Skrivervik, “ New microwave sensor for on-line blade tip timingin gas and steam turbines,”in Proceedings of the 2012 Asia-Pacific Microwave Conference (APMC 2012)Kaohsiung, Taiwan, pp.1055–1057,4–7 December 2012.

[19] MaddalenaVioletti, Jean Francois Zurcher, Jonathan Geisheimer and Anja K. Skrivervik, ”Design of antenna based sensors for blade tip clearance measurement in gas turbines,” in IEEE Conference Publications,Barcelona,Spain ,pp.1-4 2010.

[20] Aline Katharina Zimmer, ”Investigation of the impact of turbine blade geometry on near-field microwave blade tip time of arrival measurements,” M.S dissertation, Daniel Guggenheim School of Aerospace Engineering, Georgia Institute of Technology, December 2008.

[21] M. Violetti, A. K. Skrivervik, Q. Xu, J. Geisheimer, and G. Egger, “Device and method for monitoring rotor blades of a turbine,” European Patent Application No. 11181622, Sept. 16, 2011.

[22] RyszardSzczepanik, RadoslawPrzysowa, JaroslawSpychala, Edward Rokicki, Krzysztof Kamierczak and Pawel Majewski, ” Application of blade tip sensors to blade vibration monitoring in gas turbines,” in ThermalPowerPlants, Poland Air Force Institute of Technology, pp.145-175, 2012.

[23] Azharshadab, Lokeshkumar , Mohit Kumar, KamalKishor, Akash SethiandIla Sharma,” comparative analysis of rectangular and circular waveguide using matlab simulation, ”International Journal of Distributed and Parallel Systems (IJDPS) Vol.3, No.4, July 2012.

[24] Peter A. Rizzi, ”Microwave resonator and filters,” in Microwave engineering passive circuits, Latest Edition, pp. 427-438, 2004.

[25] Leonard C. Maier and J. C. Slater, "Field Strength Measurements in Resonant Cavities, "Journal of Applied Physics, vol. 23,issus.1, 15 June 2004.

[26] M.A. Hejazi, G.B. Gharehpetian, G. Moradi, H.A. Alehosseini1 and M. Mohammadi, ”Online monitoring of transformer winding axial displacement and its extent using scattering parameters and k-nearest neighbour method,” IET Gen. Trans& Distribution, Vol. 5, pp. 824 - 832, August 2011.